

Origin of the anomalous Hall effect in two-band chiral superconductors

M. D. E. Denys* and P. M. R. Brydon[†]

*Department of Physics and MacDiarmid Institute for Advanced Materials and Nanotechnology,
University of Otago, PO Box 56, Dunedin 9054, New Zealand*

 (Received 1 November 2020; revised 16 February 2021; accepted 17 February 2021; published 4 March 2021)

We consider the origin of the anomalous Hall effect in a general model of a clean two-band chiral superconductor. Within the Kubo formalism we derive an analytic expression for the high-frequency ac Hall conductivity valid close to the critical temperature. This expression involves two distinct gauge-invariant time-reversal-odd bilinear (TROB) functions involving the pairing potential and its Hermitian conjugate. We argue that the existence of at least one of these TROBs generically implies a nonzero ac Hall conductivity. The TROBs allow us to clarify the roles of intra- and interband pairing, and provide a straightforward criterion for a superconducting state to exhibit the anomalous Hall effect. We briefly exemplify our results with model calculations of two different chiral p -wave pairing states in strontium ruthenate and a chiral d -wave pairing state on the honeycomb lattice.

DOI: [10.1103/PhysRevB.103.094503](https://doi.org/10.1103/PhysRevB.103.094503)

I. INTRODUCTION

Chiral superconductivity is an exotic pairing state characterized by the spontaneous breaking of time-reversal symmetry and a handed winding of the gap phase around the Fermi surface [1]. Chiral pairing states have been proposed for a number of superconductors, most notably Sr_2RuO_4 [2], UPt_3 [3,4], URu_2Si_2 [5], and twisted bilayer graphene [6], although a definitive interpretation of the experimental evidence remains elusive. The observation of the polar Kerr effect, which is closely related to the anomalous Hall effect (AHE) [7,8], is a key signature of time-reversal symmetry breaking (TRSB) in the bulk. Indeed, a nonzero Kerr signal has been observed in various candidate superconductors, such as Sr_2RuO_4 [9], UPt_3 [10], URu_2Si_2 [11], Bi/Ni bilayers [12], $\text{PrO}_4\text{Sb}_{12}$ [13], and UTe_2 [14], providing strong evidence for the presence of chiral pairing states in these materials.

The origin of the polar Kerr effect in a chiral superconductor has been the subject of much debate, as the breaking of time-reversal symmetry by the pairing potential is not sufficient to explain the presence of the AHE. Specifically, in chiral superconductors time-reversal symmetry is broken in the relative momentum coordinate of the Cooper pair, while it is the center-of-mass coordinate that couples to the external electric field in the AHE [1,15]. Thus, the AHE is vanishing in single-band superconductors except in the presence of impurities that break the translational symmetry, which necessitates that these coordinates are independent [16–20]. On the other hand, the relative and center-of-mass coordinates are coupled in multiband superconductors [15], so mechanisms intrinsic to the clean superconductor can contribute to the AHE. Such an intrinsic contribution has been theoretically demonstrated

in a large number of models [15,21–28]. Nevertheless, it is unclear what conditions the pairing potential in a multiband model should satisfy for the existence of the AHE.

Within a simple model of chiral d -wave pairing on the honeycomb lattice, Ref. [27] identified a TRSB bilinear combination of the pairing potential and its Hermitian conjugate as critical to the appearance of the AHE. Dubbed the “time-reversal-odd bilinear” (TROB), this quantity is explicitly gauge invariant and breaks time-reversal symmetry by construction. Although the simplicity of the model studied in Ref. [27] made the wider relevance of the TROB uncertain, the authors speculated that a nonzero TROB is crucial for the existence of an intrinsic AHE in a multiband chiral superconductor. In this paper we demonstrate that this is indeed the case by analytically calculating the ac Hall conductivity for a generic model of a two-band superconductor. Our work establishes general conditions on the form of the pairing potential required for the existence of a TROB.

We begin in Sec. II by introducing a general model of a two-band system where the normal state Hamiltonian includes all terms allowed by inversion and time-reversal symmetry. Using the Kubo formalism, in Sec. III we analytically determine the leading contribution to the ac Hall conductivity in the limit of high frequencies and a small gap, revealing that the Hall conductivity depends upon two distinct TROBs. We evaluate these TROBs for arbitrary even- and odd-parity pairing states in Sec. III A, which reveals the general importance of interband pairing, but suggests that purely intraband pairing may also play a role. Although our analysis is performed in an asymptotic limit, we argue in Sec. III B that our conclusions should hold more generally. Our analysis is made concrete in Sec. IV by considering two model systems: chiral p -wave pairing in Sr_2RuO_4 (considering both E_u [15] and $B_{1u} + iB_{2u}$ pairing states) and d -wave superconductivity on the honeycomb lattice [27]. Finally, we conclude in Sec. V with an outlook for future work.

*mathew.denys@postgrad.otago.ac.nz

[†]philip.brydon@otago.ac.nz

II. MODEL

We consider a general superconducting system in which the electronic states are described by their momentum, spin, and an additional discrete degree of freedom, which we denote as the orbital. In a model with two orbitals the single-particle Hamiltonian is written in the Bogoliubov-de Gennes (BdG) formalism as

$$\mathcal{H} = \frac{1}{2} \sum_{\mathbf{k}} \Psi_{\mathbf{k}}^{\dagger} \begin{pmatrix} H_0(\mathbf{k}) & \Delta(\mathbf{k}) \\ \Delta^{\dagger}(\mathbf{k}) & -H_0^T(-\mathbf{k}) \end{pmatrix} \Psi_{\mathbf{k}}, \quad (1)$$

where

$$\Psi_{\mathbf{k}} = \begin{pmatrix} \hat{\mathbf{a}}_{\mathbf{k}} \\ \hat{\mathbf{a}}_{-\mathbf{k}}^* \end{pmatrix} \quad (2)$$

with

$$\hat{\mathbf{a}}_{\mathbf{k}}^T = (\hat{a}_{\mathbf{k},1,\uparrow}, \hat{a}_{\mathbf{k},1,\downarrow}, \hat{a}_{\mathbf{k},2,\uparrow}, \hat{a}_{\mathbf{k},2,\downarrow}), \quad (3)$$

and $\hat{a}_{\mathbf{k},\eta,\sigma}$ the annihilation operator for an electron with momentum \mathbf{k} and spin σ in the orbital η . Both H_0 and Δ are 4×4 matrices in the combined orbital-spin space, and transform under inversion \mathcal{I} and time reversal Θ as

$$\mathcal{I} : H_0(\mathbf{k}) = U_I^{\dagger} H_0(-\mathbf{k}) U_I = H_0(\mathbf{k}), \quad (4)$$

$$\mathcal{I} : \Delta(\mathbf{k}) = U_I^{\dagger} \Delta(-\mathbf{k}) U_I^* = \pm \Delta(\mathbf{k}), \quad (5)$$

$$\Theta : H_0(\mathbf{k}) = U_T^{\dagger} H_0^*(-\mathbf{k}) U_T = H_0(\mathbf{k}), \quad (6)$$

$$\Theta : \Delta(\mathbf{k}) = U_T^{\dagger} \Delta^*(-\mathbf{k}) U_T^* \neq \Delta(\mathbf{k}), \quad (7)$$

where U_I and U_T are unitary matrices. Whereas the normal state Hamiltonian H_0 is assumed to be symmetric under both spatial inversion and time reversal, the pairing potential $\Delta(\mathbf{k})$ is assumed to have definite parity but breaks time-reversal symmetry. Although the derivation in Sec. III proceeds identically for mixed-parity pairing states, we ignore this case here since it typically requires broken inversion symmetry in the normal state.

The normal state Hamiltonian matrix can be decomposed as

$$H_0(\mathbf{k}) = \sum_{\alpha,\beta=0}^3 h_{\alpha\beta}(\mathbf{k}) \eta_{\alpha} \otimes \sigma_{\beta}, \quad (8)$$

where η_{α} (σ_{β}) are Pauli matrices encoding the orbital (spin) degree of freedom. Hermiticity requires the $h_{\alpha\beta}(\mathbf{k})$ coefficients to be real valued, while the presence of inversion and time reversal permit just six (α, β) pairs in Eq. (8). These correspond to five mutually anticommuting matrices $\gamma_{1\dots 5}$, along with the identity matrix $\mathbb{1}_4 = \eta_0 \otimes \sigma_0$. The particular form of the matrices γ_i depends on the system under consideration. For example, a system with two orbitals of the same parity has $U_I = \mathbb{1}_4$ and $U_T = \eta_0 \otimes i\sigma_2$, and the allowed terms in Eq. (8) are

$$(\alpha, \beta) = (0, 0), (1, 0), (3, 0), (2, 1), (2, 2), (2, 3). \quad (9)$$

For a system with orbitals exchanged by inversion symmetry such that $U_I = \eta_1 \otimes \sigma_0$ and $U_T = \eta_0 \otimes i\sigma_2$, the allowed terms are

$$(\alpha, \beta) = (0, 0), (1, 0), (2, 0), (3, 1), (3, 2), (3, 3). \quad (10)$$

TABLE I. The (α, β) terms permitted in Eq. (8) for systems with each possible form of inversion and time reversal, enumerated by the orbital parts of U_I and U_T . In each case the allowed terms correspond to the identity along with five mutually anticommuting matrices. $U_T^{[\alpha]} = \eta_2$ is not allowed as it leads to $U_T U_T^* = +\mathbb{1}$, which does not correspond to a spin-half system. We exclude cases where inversion does not commute with time-reversal (i.e., $U_I U_T \neq U_T U_I^*$) and where the inversion operator is not its own inverse (i.e., $U_I U_I \neq \mathbb{1}$).

$U_I^{[\alpha]}$	$U_T^{[\alpha]}$	Allowed (α, β) terms
η_0	η_0	(0,0), (1,0), (3,0), (2,1), (2,2), (2,3)
	η_1	(0,0), (1,0), (2,0), (3,1), (3,2), (3,3)
	η_3	(0,0), (2,0), (3,0), (1,1), (1,2), (1,3)
η_1	η_0	(0,0), (1,0), (2,0), (3,1), (3,2), (3,3)
	η_1	(0,0), (1,0), (3,0), (2,1), (2,2), (2,3)
η_2	η_1	(0,0), (2,0), (3,0), (1,1), (1,2), (1,3)
	η_3	(0,0), (1,0), (2,0), (3,1), (3,2), (3,3)
η_3	η_0	(0,0), (2,0), (3,0), (1,1), (1,2), (1,3)
	η_3	(0,0), (1,0), (3,0), (2,1), (2,2), (2,3)

All other possibilities are summarized in Table I. Although some of these may appear atypical, they can each be related to one of the cases noted above via a canonical transformation.

It is convenient to rewrite the normal state Hamiltonian as

$$H_0(\mathbf{k}) = h_{00}(\mathbf{k}) \mathbb{1}_4 + \mathbf{h}(\mathbf{k}) \cdot \boldsymbol{\gamma}, \quad (11)$$

where $h_{00}(\mathbf{k})$ is an even function of momentum, $\boldsymbol{\gamma} = (\gamma_1, \dots, \gamma_5)$ is a vector of the γ matrices, and $\mathbf{h}(\mathbf{k}) = (h_{\alpha_1\beta_1}, \dots, h_{\alpha_5\beta_5})$ is a vector of the corresponding coefficients. For future reference we define the flattened normal state Hamiltonian

$$\tilde{H}_0(\mathbf{k}) = \frac{H_0(\mathbf{k}) - h_{00}(\mathbf{k}) \mathbb{1}_4}{|\mathbf{h}(\mathbf{k})|} = \hat{\mathbf{h}}(\mathbf{k}) \cdot \boldsymbol{\gamma}, \quad (12)$$

where $\hat{\mathbf{h}} = \mathbf{h}/|\mathbf{h}|$. This is traceless and satisfies the eponymous property

$$\tilde{H}_0(\mathbf{k}) |\mathbf{k}, \pm, s\rangle = \pm |\mathbf{k}, \pm, s\rangle, \quad (13)$$

where $|\mathbf{k}, \pm, s\rangle$ are eigenstates of H_0 with the good quantum numbers momentum \mathbf{k} , band \pm , and pseudospin s . The existence of a degenerate pseudospin index is guaranteed by the inversion and time-reversal symmetries [29,30].

Analogously to Eq. (8), the pairing potential Δ can be decomposed in terms of orbital and spin Pauli matrices, but its form is not so restricted because inversion and time-reversal symmetries can be broken in the superconducting state. We only enforce that the potential satisfies fermionic antisymmetry, requiring that $\Delta(\mathbf{k}) = -\Delta^T(-\mathbf{k})$. For convenience, we define the transformed pairing potential

$$\tilde{\Delta}(\mathbf{k}) = \Delta(\mathbf{k}) U_T^{\dagger}, \quad (14)$$

which transforms analogously to H_0 under point symmetry operations, and has the useful property that $\tilde{\Delta}$ and $\tilde{\Delta}^{\dagger}$ are time-reversed counterparts. Although the particular form of $\tilde{\Delta}(\mathbf{k})$ is set by the details of the system, we note that for an even-parity pairing state it will be a linear combination of the six $\eta_{\alpha} \otimes \sigma_{\beta}$ matrices which are allowed to appear in the normal state Hamiltonian; the potential for an odd-parity pairing state will involve the other ten matrices.

III. HALL CONDUCTIVITY AND TIME-REVERSAL-ODD BILINEARS

The frequency-dependent Hall conductivity is defined as

$$\sigma_H(\omega) = \frac{i}{2\omega} \lim_{i\omega_n \rightarrow \omega + i0^+} [\pi_{xy}(i\omega_n) - \pi_{yx}(i\omega_n)], \quad (15)$$

where π_{ab} is the current-current correlation function [31]

$$\pi_{ab}(i\omega_n) = -\frac{1}{N} \int_0^\beta d\tau e^{i\omega_n \tau} \langle T_\tau J_a(\tau) J_b(0) \rangle, \quad (16)$$

N is the number of lattice points in the crystal, τ is the imaginary time, J_a is the a th component of the current operator

$$J_a = e \sum_k \Psi_k^\dagger v_k^a \Psi_k, \quad (17)$$

and the velocity matrix v_k^a is given by

$$v_k^a = \begin{pmatrix} v_k^{ea} & 0 \\ 0 & v_k^{ha} \end{pmatrix} = \begin{pmatrix} \frac{\partial H_0(\mathbf{k})}{\partial k_a} & 0 \\ 0 & \frac{\partial (-H_0^T(-\mathbf{k}))}{\partial k_a} \end{pmatrix}. \quad (18)$$

In the linear response regime $\pi_{ab}(i\omega_n)$ is evaluated at the one-loop level, yielding

$$\pi_{ab}(i\omega_n) = \frac{e^2}{2N\beta} \sum_{k,m} \text{Tr} \{ v_k^a \mathcal{G}_{k,i\omega_n + iv_m} v_k^b \mathcal{G}_{k,iv_m} \}, \quad (19)$$

where \mathcal{G}_{k,iv_m} is the Matsubara Green's function corresponding to Eq. (1). Note that in Eq. (19) $\omega_n = 2n\pi/\beta$ is a bosonic Matsubara frequency, and $\nu_m = (2m+1)\pi/\beta$ is a fermionic Matsubara frequency. For convenience we set $\hbar = 1$.

While Eq. (19) can be evaluated for an arbitrary pairing potential, the resulting analytic expression is generally very complicated and offers only limited insight. Progress can be made by considering the high-frequency, small-gap limit, obtained by neglecting terms in Eq. (19) of lower order than ω^{-2} and higher order than $|\Delta|^2$. This choice is justified since experiments are often performed in the high-frequency regime, and the gap is small compared to other relevant energy scales; the small-gap approximation is expected to be particularly accurate close to the critical temperature. Performing a diagrammatic expansion of Eq. (19), an approximate expression for the intrinsic anomalous Hall conductivity in this limit is given by [27]

$$\sigma_H(\omega) \approx \frac{ie^2}{2N\omega^2\beta} \sum_{k,m} \text{Tr} \{ [v \wedge v] \mathcal{G}_0 H_\Delta \mathcal{G}_0 H_\Delta \mathcal{G}_0 \}, \quad (20)$$

where $[a \wedge b] = a^x b^y - a^y b^x$, and explicit momentum and frequency indices have been dropped for convenience. H_Δ is the

pairing part of the BdG Hamiltonian,

$$H_{\Delta,\mathbf{k}} = \begin{pmatrix} 0 & \Delta(\mathbf{k}) \\ \Delta^\dagger(\mathbf{k}) & 0 \end{pmatrix}, \quad (21)$$

and $\mathcal{G}_0 = \mathcal{G}_{0,k,iv_m}$ is the normal state Matsubara Green's function in the Nambu representation

$$\mathcal{G}_{0,k,iv_m} = \begin{pmatrix} \mathcal{G}_{0,k,iv_m}^e & 0 \\ 0 & \mathcal{G}_{0,k,iv_m}^h \end{pmatrix}. \quad (22)$$

With these expressions, the trace in Eq. (20) is split into two terms. By enforcing that H_0 is symmetric under both inversion and time reversal, and noting that time reversal commutes with inversion (i.e., $U_I U_T = U_T U_I^*$, as time reversal is antiunitary), it can be shown that $[v^h \wedge v^h] = -U_I^T [v^e \wedge v^e] U_I^*$ and $U_I^\dagger U_T^\dagger [v^e \wedge v^e]^T U_T U_I = -[v^e \wedge v^e]$, from which we obtain

$$\begin{aligned} \sigma_H(\omega) \approx & \frac{ie^2}{2N\omega^2\beta} \sum_{k,m} [\text{Tr} \{ [v^e \wedge v^e] \mathcal{G}_0^e \tilde{\Delta} U_T \mathcal{G}_0^h U_T^\dagger \tilde{\Delta}^\dagger \mathcal{G}_0^e \} \\ & + \text{Tr} \{ [v^e \wedge v^e] U_T^\dagger \mathcal{G}_0^h U_T \tilde{\Delta}^\dagger \mathcal{G}_0^e \tilde{\Delta} U_T^\dagger \mathcal{G}_0^h U_T \}] \end{aligned} \quad (23)$$

in the high-frequency, small-gap limit. The electronlike Green's functions can be written in terms of projection operators onto each normal state energy band:

$$\mathcal{G}_{0,k,iv_m}^e = \sum_{\pm} \frac{\mathcal{P}_{k,\pm}}{iv_m - E_{k,\pm}}. \quad (24)$$

The projection operators are defined in terms of Eq. (12) as $\mathcal{P}_{k,\pm} = [\mathbb{1} \pm \tilde{H}_0(\mathbf{k})]/2$, and therefore

$$\begin{aligned} \mathcal{G}_{0,k,iv_m}^e &= \frac{\mathbb{1} + \tilde{H}_0(\mathbf{k})}{2(iv_m - E_{k,+})} + \frac{\mathbb{1} - \tilde{H}_0(\mathbf{k})}{2(iv_m - E_{k,-})} \\ &= a_{k,\nu_m} \mathbb{1} + b_{k,\nu_m} \tilde{H}_0(\mathbf{k}), \end{aligned} \quad (25)$$

where

$$a_{k,\nu_m} = \frac{1}{2} [(iv_m - E_{k,+})^{-1} + (iv_m - E_{k,-})^{-1}], \quad (26)$$

$$b_{k,\nu_m} = \frac{1}{2} [(iv_m - E_{k,+})^{-1} - (iv_m - E_{k,-})^{-1}]. \quad (27)$$

Analogously, the holelike Green's function has the form

$$\mathcal{G}_{0,k,iv_m}^h = c_{k,\nu_m} \mathbb{1} + d_{k,\nu_m} \tilde{H}_0^T(-\mathbf{k}), \quad (28)$$

where $c_{k,\nu_m} = -a_{k,-\nu_m}$ and $d_{k,\nu_m} = -b_{k,-\nu_m}$. Further, because H_0 is symmetric under time reversal,

$$U_T^\dagger \mathcal{G}_{0,k,iv_m}^h U_T = c_{k,\nu_m} \mathbb{1} + d_{k,\nu_m} \tilde{H}_0(\mathbf{k}). \quad (29)$$

Substituting Eq. (25) and Eq. (29) into Eq. (23), and using the relationship between a_{k,ν_m} (b_{k,ν_m}) and c_{k,ν_m} (d_{k,ν_m}), we obtain after some manipulation

$$\begin{aligned} \sigma_H(\omega) = & \frac{ie^2}{2N\omega^2\beta} \sum_{k,m} [a^2 c \text{Tr} \{ [v^e \wedge v^e] \text{TROB}_1 \} + b^2 c \text{Tr} \{ \tilde{H}_0 [v^e \wedge v^e] \tilde{H}_0 \text{TROB}_1 \} + abc \text{Tr} \{ \tilde{H}_0, [v^e \wedge v^e] \} \text{TROB}_1] \\ & + a^2 d \text{Tr} \{ [v^e \wedge v^e] \text{TROB}_2 \} + b^2 d \text{Tr} \{ \tilde{H}_0 [v^e \wedge v^e] \tilde{H}_0 \text{TROB}_2 \} + abd \text{Tr} \{ \{ \tilde{H}_0, [v^e \wedge v^e] \} \} \text{TROB}_2], \end{aligned} \quad (30)$$

where momentum and frequency indices are suppressed for clarity. The key feature of Eq. (30) is the introduction of two distinct time-reversal-odd bilinears (TROBs), which are defined in terms of the pairing potential:

$$\text{TROB}_1 \equiv \tilde{\Delta} \tilde{\Delta}^\dagger - \tilde{\Delta}^\dagger \tilde{\Delta}, \quad (31)$$

$$\text{TROB}_2 \equiv \tilde{\Delta} \tilde{H}_0 \tilde{\Delta}^\dagger - \tilde{\Delta}^\dagger \tilde{H}_0 \tilde{\Delta}. \quad (32)$$

TROB_1 was initially introduced in Ref. [27]. It can be verified that both TROBs are the difference of a gauge-invariant quantity and its time-reversed value, making them odd under time reversal by construction. The significance of the TROBs is that they translate the TRSB in the particle-particle channel to the observable particle-hole channel.

This direct dependence of the anomalous Hall conductivity on TROBs is the core result of this paper. We observe that the presence of at least one nonvanishing TROB is a necessary condition for a nonzero Hall conductivity in the high-frequency, small-gap limit. Although this is not a sufficient condition, fine tuning is required for Eq. (30) to be vanishing if either TROB is nonzero. Importantly, although the TROBs are only nonzero for a TRSB pairing potential, a vanishing TROB does not imply that the pairing potential is time-reversal symmetric. As such, the TROBs significantly constrain which superconducting states can give rise to a nonzero anomalous Hall conductivity. Both TROBs are straightforward to calculate, and hence provide an easy mechanism for identifying candidate Hamiltonians worth further examination.

Another important aspect of Eq. (30) is the presence of the wedge product of velocity matrices [$v^e \wedge v^e$]. Since this product is vanishing in a single-band system, it implies that a multiband model is necessary for an anomalous Hall conductivity.

A. Interband vs intraband pairing

Interband pairing has been identified by a number of authors as another necessary condition for an AHE [15,27]. This is notable because intraband pairing generally guarantees the robustness of the superconducting instability, while interband pairing competes, and is therefore detrimental to the formation of a superconducting state [32]. The connection between, and compatibility of, these claims and our result is of interest, and while Eq. (30) must be basis independent because the Hall conductivity is an observable, we can cast the TROBs in a band-pseudospin basis. By doing so, we show that the TROBs directly evidence the key role played by interband pairing, while also demonstrating that purely intraband pairing can generate a nonzero Hall conductivity.

1. Even-parity pairing

The general form of an even-parity pairing potential in the band-pseudospin basis is

$$\tilde{\Delta}_e = \frac{1}{2}(\psi_+ + \psi_-)b_0 \otimes s_0 + \frac{1}{2}(\psi_+ - \psi_-)b_3 \otimes s_0 + \psi_e b_1 \otimes s_0 + \mathbf{d}_e \cdot (b_2 \otimes \mathbf{s}), \quad (33)$$

where the first line describes intraband pseudospin-singlet pairing with potential ψ_\pm in band \pm , while ψ_e and \mathbf{d}_e are the interband pseudospin-singlet and -triplet potentials. The

Pauli matrices b_μ and s_μ encode the band and pseudospin degrees of freedom, respectively, and all pairing potentials are even functions of the momentum. Because the pseudospin and band indices are even under inversion, the inversion operator is trivial in this representation, and so the matrices appearing in Eq. (33) are essentially the same as in the case of Eq. (9). The two TROBs evaluate as

$$\begin{aligned} \text{TROB}_1 &= 2i\mathbf{d}_e \times \mathbf{d}_e^* \cdot (b_0 \otimes \mathbf{s}) - 4\Im\{\psi_e \mathbf{d}_e^*\} \cdot (b_3 \otimes \mathbf{s}) \\ &\quad - 2\Im\{(\psi_+ - \psi_-)\psi_e^*\} b_2 \otimes s_0 \\ &\quad + 2\Im\{(\psi_+ - \psi_-)\mathbf{d}_e^*\} \cdot (b_1 \otimes \mathbf{s}), \end{aligned} \quad (34)$$

$$\begin{aligned} \text{TROB}_2 &= -2i\mathbf{d}_e \times \mathbf{d}_e^* \cdot (b_3 \otimes \mathbf{s}) + 4\Im\{\psi_e \mathbf{d}_e^*\} \cdot (b_0 \otimes \mathbf{s}) \\ &\quad - 2\Im\{(\psi_+ + \psi_-)\psi_e^*\} b_2 \otimes s_0 \\ &\quad + 2\Im\{(\psi_+ + \psi_-)\mathbf{d}_e^*\} \cdot (b_1 \otimes \mathbf{s}). \end{aligned} \quad (35)$$

We observe that the pairing potential must have interband components for either TROB to be nonzero, which is generically the case if the pairing potential has a nontrivial matrix structure when expressed in the orbital-spin basis. Note that the velocity operators are not generally diagonal in the band-pseudospin picture, and so the off-diagonal components of the TROBs are still relevant to the existence of the Hall conductivity. We note that the diagonal blocks of TROB_1 also play a crucial role in the inflation of point or line nodes into Bogoliubov Fermi surfaces [33].

2. Odd-parity pairing

Adopting the same band-pseudospin basis as above, a general odd-parity pairing potential has the form

$$\begin{aligned} \tilde{\Delta}_o &= \frac{1}{2}(\mathbf{d}_+ + \mathbf{d}_-) \cdot (b_0 \otimes \mathbf{s}) + \frac{1}{2}(\mathbf{d}_+ - \mathbf{d}_-) \cdot (b_3 \otimes \mathbf{s}) \\ &\quad + \psi_o b_2 \otimes s_0 + \mathbf{d}_o \cdot (b_1 \otimes \mathbf{s}), \end{aligned} \quad (36)$$

where in addition to the intraband triplet potentials \mathbf{d}_\pm there are also interband singlet ψ_o and triplet \mathbf{d}_o potentials. Here all potentials are odd in momentum. Evaluating the TROBs we obtain

$$\begin{aligned} \text{TROB}_1 &= i\mathbf{d}_+ \times \mathbf{d}_+^* \cdot ([b_0 + b_3] \otimes \mathbf{s}) \\ &\quad + i\mathbf{d}_- \times \mathbf{d}_-^* \cdot ([b_0 - b_3] \otimes \mathbf{s}) \\ &\quad + 2i\mathbf{d}_o \times \mathbf{d}_o^* \cdot (b_0 \otimes \mathbf{s}) + 4\Im\{\psi_o \mathbf{d}_o^*\} \cdot (b_3 \otimes \mathbf{s}) \\ &\quad + 2\Im\{\mathbf{d}_o \cdot [\mathbf{d}_+ - \mathbf{d}_-]^*\} b_2 \otimes s_0 \\ &\quad - 2\Im\{\mathbf{d}_o \times [\mathbf{d}_+ + \mathbf{d}_-]^*\} \cdot (b_1 \otimes \mathbf{s}), \\ &\quad - 2\Im\{\psi_o [\mathbf{d}_+ - \mathbf{d}_-]^*\} \cdot (b_1 \otimes \mathbf{s}) \end{aligned} \quad (37)$$

$$\begin{aligned} \text{TROB}_2 &= i\mathbf{d}_+ \times \mathbf{d}_+^* \cdot ([b_0 + b_3] \otimes \mathbf{s}) \\ &\quad - i\mathbf{d}_- \times \mathbf{d}_-^* \cdot ([b_0 - b_3] \otimes \mathbf{s}) \\ &\quad + 2i\mathbf{d}_o \times \mathbf{d}_o^* \cdot (b_3 \otimes \mathbf{s}) - 4\Im\{\psi_o \mathbf{d}_o^*\} \cdot (b_0 \otimes \mathbf{s}) \\ &\quad + 2\Im\{\mathbf{d}_o \cdot [\mathbf{d}_+ + \mathbf{d}_-]^*\} b_2 \otimes s_0 \\ &\quad - 2\Im\{\mathbf{d}_o \times [\mathbf{d}_+ - \mathbf{d}_-]^*\} \cdot (b_1 \otimes \mathbf{s}) \\ &\quad - 2\Im\{\psi_o [\mathbf{d}_+ + \mathbf{d}_-]^*\} \cdot (b_1 \otimes \mathbf{s}). \end{aligned} \quad (38)$$

We observe that interband pairing still plays an important role, but in contrast to the even-parity case, a purely intraband potential can give rise to a nonzero TROB if $\mathbf{d}_\pm \times \mathbf{d}_\pm^* \neq 0$.

Although such nonunitary pairing states are generically realized in TRSB single-band systems, the wedge product of velocity matrices in Eq. (30) is nevertheless only nonzero in a multiband system, reiterating the necessity of multiple bands for an anomalous Hall conductivity.

B. Away from the high-frequency, small-gap limit

Although Eq. (30) only rigorously applies in the high-frequency, small-gap limit, the conclusion that a nonzero TROB implies a nonzero Hall conductivity is generically valid, since any correction terms are unlikely to exactly cancel the leading-order contribution Eq. (30). In considering the converse statement, we start by noting that the high-frequency limit can be rigorously defined in terms of the commutator of the current operators

$$\sigma_H(\omega) \approx \frac{i}{N\omega^2} \langle [J_x, J_y] \rangle. \quad (39)$$

Note that this expression does not require the small-gap restriction. We can identify the sum in Eq. (30) as the small-gap approximation of the expectation value in Eq. (39). This expectation value also appears in a sum rule for the imaginary part of the Hall conductivity

$$\int_{-\infty}^{\infty} \omega \Im \sigma_H(\omega) d\omega = -\frac{i\pi}{N} \langle [J_x, J_y] \rangle. \quad (40)$$

The expectation value in Eq. (40) is unlikely to be zero unless the Hall conductivity itself is vanishing at all frequencies. Further, for the expectation value to be nonzero when both TROBs are vanishing implies that the leading contributions to Eq. (39) and Eq. (40) must be fourth order or higher in the pairing potential; for these higher-order contributions to be nonzero but the second-order contribution to vanish places extremely stringent conditions on both the pairing potential and the normal state Hamiltonian, which would not generically be satisfied. We thus consider it likely that vanishing

TROBs imply a vanishing Hall conductivity in a clean system at arbitrary frequency and temperature.

IV. EXAMPLE CALCULATIONS

To exemplify the role of the TROBs, here we present calculations for two model systems.

A. Strontium ruthenate

Strontium ruthenate (Sr_2RuO_4) is a key candidate material for chiral superconductivity, with both muon spin relaxation [34] and polar Kerr experiments [8,9] providing strong evidence of TRSB in its superconducting state. The theory of the anomalous Hall effect in Sr_2RuO_4 has been considered by several authors [15,21,22], all working on the assumption that it is a chiral p -wave superconductor [35–37]. Although recent experiments have thrown significant doubt on this proposition [38,39], we nevertheless adopt this picture in order to make contact with the existing literature. We follow Ref. [15] and adopt a minimal two-dimensional model of Sr_2RuO_4 involving the ruthenium d_{xz} and d_{yz} orbitals. Since the orbitals transform trivially under inversion and time reversal, Eq. (9) enumerates the terms permitted in H_0 . We take the following tight-binding model: $h_{00} = -t_1(\cos k_x + \cos k_y) - \mu$, $h_{10} = 2t_3 \sin k_x \sin k_y$, $h_{30} = -t_2(\cos k_x - \cos k_y)$, and isotropic spin orbit coupling $h_{23} = \lambda$; the (2,1) and (2,2) terms do not appear in this two-dimensional model because h_{21} and h_{22} are odd under reflection about the $k_z = 0$ mirror plane. Setting $t_1 = 1$, $\mu = 1$, $t_2 = 0.8$, $t_3 = 0.1$, and $\lambda = 0.25$, this model qualitatively reproduces the observed α and β Fermi surfaces [40–42].

We focus on pairing states belonging to the E_u irreducible representation of the D_{4h} point group, which, being two dimensional, naturally occur in TRSB combinations. A general E_u pairing state is decomposed in the orbital-spin basis as $\tilde{\Delta} = \tilde{\Delta}_{03}\eta_0 \otimes \sigma_3 + \tilde{\Delta}_{13}\eta_1 \otimes \sigma_3 + \tilde{\Delta}_{20}\eta_2 \otimes \sigma_0 + \tilde{\Delta}_{33}\eta_3 \otimes \sigma_3$, where each $\tilde{\Delta}_{\alpha\beta}$ is an odd chiral function of momentum. Note that the pairing potential that appears in the BdG Hamiltonian, Eq. (1), has the form $\Delta = \tilde{\Delta}U_T$, where $U_T = \eta_0 \otimes i\sigma_2$ for this model. The TROBs evaluate as

$$\text{TROB}_1 = 4[\Im\{\tilde{\Delta}_{13}\tilde{\Delta}_{33}^*\}\eta_2 \otimes \sigma_0 + \Im\{\tilde{\Delta}_{33}\tilde{\Delta}_{20}^*\}\eta_1 \otimes \sigma_3 + \Im\{\tilde{\Delta}_{20}\tilde{\Delta}_{13}^*\}\eta_3 \otimes \sigma_3], \quad (41)$$

$$\begin{aligned} \text{TROB}_2 = & 4[(\hat{h}_{10}\Im\{\tilde{\Delta}_{20}\tilde{\Delta}_{33}^*\} + \hat{h}_{30}\Im\{\tilde{\Delta}_{11}\tilde{\Delta}_{22}^*\} + \hat{h}_{23}\Im\{\tilde{\Delta}_{33}\tilde{\Delta}_{13}^*\})\eta_0 \otimes \sigma_3 \\ & + (\hat{h}_{30}\Im\{\tilde{\Delta}_{03}\tilde{\Delta}_{20}^*\} + \hat{h}_{23}\Im\{\tilde{\Delta}_{33}\tilde{\Delta}_{03}^*\})\eta_1 \otimes \sigma_3 + (\hat{h}_{10}\Im\{\tilde{\Delta}_{03}\tilde{\Delta}_{33}^*\} + \hat{h}_{30}\Im\{\tilde{\Delta}_{13}\tilde{\Delta}_{03}^*\})\eta_2 \otimes \sigma_0 \\ & + (\hat{h}_{23}\Im\{\tilde{\Delta}_{03}\tilde{\Delta}_{13}^*\} + \hat{h}_{10}\Im\{\tilde{\Delta}_{20}\tilde{\Delta}_{03}^*\})\eta_3 \otimes \sigma_3]. \end{aligned} \quad (42)$$

In general, both TROBs are nonzero, although they can each individually vanish depending on the details of a given model. Further, each term in Eq. (41) and Eq. (42) involves two pairing channels: although chiral pairing in a single channel is sufficient to break time-reversal symmetry, pairing in at least two channels is required for the appearance of an anomalous Hall conductivity.

As a specific model for further examination we take the intraorbital spin-triplet pairing state considered in

Ref. [15]

$$\tilde{\Delta} = \tilde{\Delta}_{03}\eta_0 \otimes \sigma_3 + \tilde{\Delta}_{33}\eta_3 \otimes \sigma_3, \quad (43)$$

with the p -wave form factors $\tilde{\Delta}_{03} = \tilde{\Delta}_{0,03}(\sin k_x + i \sin k_y)$ and $\tilde{\Delta}_{33} = \tilde{\Delta}_{0,33}(\sin k_x - i \sin k_y)$. Only TROB_2 is nonzero for this system, evaluating to

$$\text{TROB}_2 = 4\Im\{\tilde{\Delta}_{03}\tilde{\Delta}_{33}^*\}(\hat{h}_{10}\eta_2 \otimes \sigma_0 - \hat{h}_{23}\eta_1 \otimes \sigma_3). \quad (44)$$

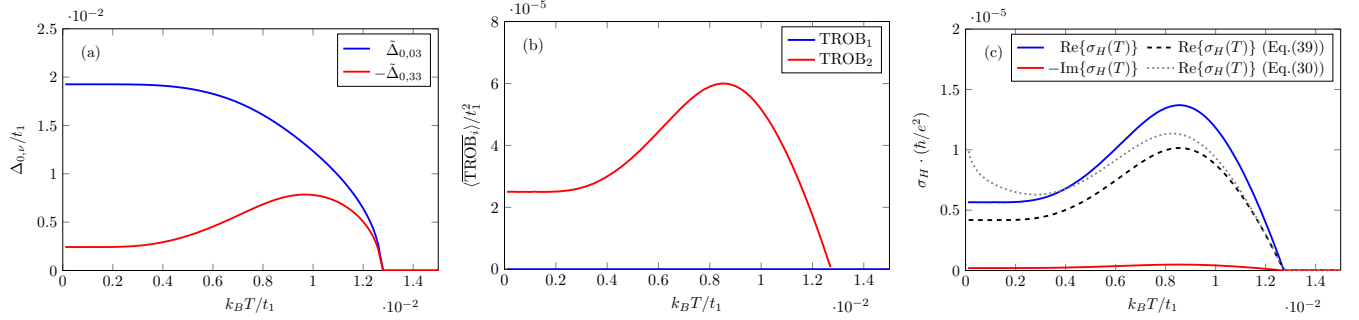


FIG. 1. (a) The pairing potential amplitudes, (b) dimensionless TROB expectation values, and (c) Hall conductivity at frequency $\omega = 2t_1$, calculated as a function of temperature for the E_u model of strontium ruthenate discussed in the text. The Hall conductivity is shown both exactly [calculated using Eq. (15) and Eq. (19)] and in its approximate forms in the high-frequency and high-frequency, small-gap limits [using Eq. (39) and Eq. (30), respectively]. Calculated with $N = 500 \times 500$ for (a) and (b), and $N = 5000 \times 5000$ for (c). The positive infinitesimal in Eq. (15) was numerically approximated as $0^+ = 0.001$.

Microscopically, TROB_2 can be interpreted as an orbital- or spin-angular-momentum-polarized interorbital hopping term.

To study the temperature dependence of the TROB, we determine the pairing potential amplitudes $\tilde{\Delta}_{0,01}$ and $\tilde{\Delta}_{0,31}$ self-consistently. To this end, we introduce a phenomenological pairing interaction $V_{\nu,\nu'}$, which scatters a Cooper pair from channel ν' to channel ν . The interaction strengths were taken to be $V_{03,03} = -0.2$, $V_{33,33} = -0.265$, and $V_{03,33} = V_{33,03} = 0.03$. These values were chosen such that $\tilde{\Delta}_{0,33}$ exhibits a nonmonotonic temperature dependence, as shown in Fig. 1(a). The existence of TROB_2 in this state is confirmed by the thermal expectation value of the dimensionless quantity $\overline{\text{TROB}}_i = \text{TROB}_i / |\tilde{\Delta}_{0,03} \tilde{\Delta}_{0,33}|$, which is shown in Fig. 1(b). The nonmonotonic temperature dependence of the TROB is particularly helpful when comparing the approximate form of the Hall conductivity Eq. (30) with the full calculation, which is shown in Fig. 1(c). We additionally include the prediction of the high-frequency limit Eq. (39). The two approximate results are in excellent qualitative agreement with the full calculation, and also in reasonable quantitative agreement; the quantitative agreement improves at higher values of the frequency. Although this underscores the fact that the small-gap approximation captures the leading contribution to the Hall conductivity, we note that this approximation appears to break down as the temperature goes to zero.

Intraband contributions

Intraband contributions to the Hall conductivity are vanishing within the E_u pairing states considered above for our model of strontium ruthenate [15]. To exemplify the role purely intraband contributions can play in the Hall conductivity, we turn to an alternative pairing potential, constructed as a chiral superposition of a B_{1u} and B_{2u} pairing state: $\tilde{\Delta} = \tilde{\Delta}_{B_{1u}} + i\tilde{\Delta}_{B_{2u}}$ with $\tilde{\Delta}_{B_{1u}} = \tilde{\Delta}_{0,B_{1u}}(\sin k_x \eta_0 \otimes \sigma_1 - \sin k_y \eta_0 \otimes \sigma_2)$ and $\tilde{\Delta}_{B_{2u}} = \tilde{\Delta}_{0,B_{2u}}(\sin k_x \eta_0 \otimes \sigma_2 + \sin k_y \eta_0 \otimes \sigma_1)$. The $\tilde{\Delta}_{0,B_{1u}}$ and $\tilde{\Delta}_{0,B_{2u}}$ amplitudes are taken to be real. Since this potential is constructed in the orbital-spin basis, we cannot easily show that this satisfies the nonunitary condition $\mathbf{d}_\pm \times \mathbf{d}_\pm^* \neq 0$. However, we can decompose Eq. (30) into its

intra- and interband contributions,

$$\sigma_H(\omega) = \frac{ie^2}{2N\omega^2\beta} \sum_{\mathbf{k},m} \{ \tilde{\sigma}^{(\text{intra})}(\mathbf{k}, \nu_m) + \tilde{\sigma}^{(\text{inter})}(\mathbf{k}, \nu_m) \}, \quad (45)$$

by explicitly writing each trace in Eq. (30) in the band-pseudospin basis. For our $B_{1u} + iB_{2u}$ model the intraband contribution takes the form

$$\begin{aligned} \tilde{\sigma}^{(\text{intra})} &= 16i\tilde{\Delta}_{0,B_{1u}}\tilde{\Delta}_{0,B_{2u}}(\sin^2 k_x + \sin^2 k_y) \\ &\times \hat{h}_{23}(\hat{h}_{10}^2 + \hat{h}_{30}^2)(v_{x,30}v_{y,10} - v_{x,10}v_{y,30}) \\ &\times \sum_{\pm} [\pm(iv_m - E_{\mathbf{k},\pm})^{-2}(iv_m + E_{\mathbf{k},\pm})^{-1}], \end{aligned} \quad (46)$$

where $v_{x,30} = \partial h_{30} / \partial k_x$, etc. Note that each term in the sum involves energies of a single band, indicating the purely intraband nature of this term. The interband contribution can be determined similarly, or by taking the difference between Eq. (46) and Eq. (30). We note that both contributions to the Hall conductivity are vanishing for this model in the absence of the spin-orbit coupling.

Numerical calculations of the intra- and interband contributions to the Hall conductivity in the high-frequency, small-gap limit are presented in Fig. 2 as a function of the spin-orbit coupling strength, h_{23} , for $\tilde{\Delta}_{0,B_{1u}} = \tilde{\Delta}_{0,B_{2u}}/3 = 10^{-3}t_1$. Not only do we observe that the purely intraband contribution is generically nonzero, but we can also identify significant regions in which intraband contributions dominate.

B. Honeycomb lattice

An example of a TRSB even-parity superconductor with a nonzero anomalous Hall conductivity is provided by the nearest-neighbor chiral d -wave pairing state on the honeycomb lattice [43,44]. The anomalous Hall conductivity of this system was analyzed in detail in Ref. [27], which included the introduction of the TROB concept. In the notation used here, the honeycomb lattice model is written as

$$H_0 = h_{00}\eta_0 \otimes \sigma_0 + h_{10}\eta_1 \otimes \sigma_0 + h_{20}\eta_2 \otimes \sigma_0, \quad (47)$$

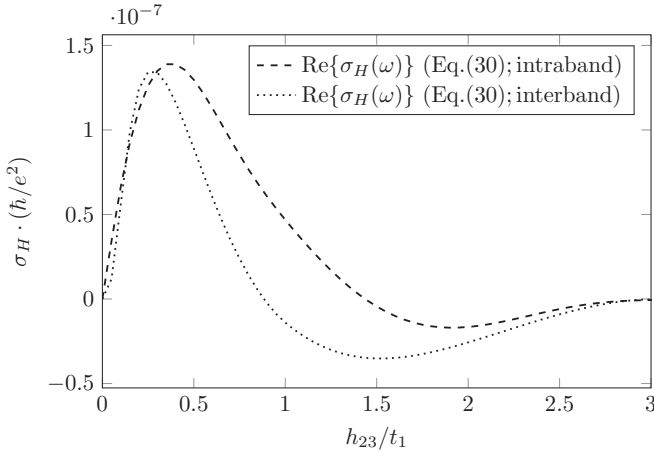


FIG. 2. The intra- and interband contributions to the Hall conductivity in the high-frequency, small-gap limit [calculated using Eq. (30) and Eq. (46)], as a function of spin-orbit coupling for the $B_{1u} + iB_{2u}$ model of strontium ruthenate discussed in the text. Calculated with $\tilde{\Delta}_{0,B_{1u}} = \tilde{\Delta}_{0,B_{2u}}/3 = 10^{-3}t_1$, $\omega = 3t_1$, $k_B T = 10^{-2}t_1$, and $N = 1000 \times 1000$.

where η_μ encodes the sublattice degree of freedom. The allowed terms are given by $h_{00} = \mu$, $h_{10} = -t(\cos k_x + 2 \cos \frac{1}{2}k_x \cos \frac{\sqrt{3}}{2}k_y)$, and $h_{20} = t(\sin k_x - 2 \sin \frac{1}{2}k_x \cos \frac{\sqrt{3}}{2}k_y)$, where μ is the chemical potential and t is the nearest-neighbor hopping. The chiral d -wave pairing potential in the irreducible representation E_{2g} of D_{6h} is written

$$\tilde{\Delta} = \tilde{\Delta}_{10}\eta_1 \otimes \sigma_0 + \tilde{\Delta}_{20}\eta_2 \otimes \sigma_0, \quad (48)$$

with the amplitudes $\tilde{\Delta}_{10} = \Delta_0(\cos k_x - \cos \frac{1}{2}k_x \cos \frac{\sqrt{3}}{2}k_y - i\sqrt{3} \sin \frac{1}{2}k_x \sin \frac{\sqrt{3}}{2}k_y)$ and $\tilde{\Delta}_{20} = -\Delta_0(\sin k_x + \sin \frac{1}{2}k_x \cos \frac{\sqrt{3}}{2}k_y + i\sqrt{3} \cos \frac{1}{2}k_x \sin \frac{\sqrt{3}}{2}k_y)$. Only TROB₁ is nonzero for this model, taking the value

$$\text{TROB}_1 = 4\Im\{\tilde{\Delta}_{10}\tilde{\Delta}_{20}^*\}\eta_3 \otimes \sigma_0. \quad (49)$$

The form of TROB₁ is equivalent to the loop current term in Haldane's model of the anomalous quantum Hall effect, and the anomalous Hall conductivity of the model is directly related to this quantity [27]. The absence of TROB₂ is an artifact of the simplicity of the model: by including the symmetry-allowed Kane-Mele spin-orbit coupling [45] $h_{33}\eta_3 \otimes \sigma_3 = \lambda \sin \frac{\sqrt{3}}{2}k_y (\cos \frac{3}{2}k_x - \cos \frac{\sqrt{3}}{2}k_y)\eta_3 \otimes \sigma_3$ in the normal state Hamiltonian, we find

$$\text{TROB}_2 = 4\hat{h}_{33}\Im\{\tilde{\Delta}_{10}^*\tilde{\Delta}_{20}\}\eta_0 \otimes \sigma_3, \quad (50)$$

while TROB₁ is left unchanged.

The TROB results for the honeycomb lattice are readily understood in terms of the band-pseudospin picture. In the absence of spin-orbit coupling, the pseudospin can be chosen as identical to the real spin, and so the interband pairing is purely singlet. Since the intraband singlet potentials have opposite sign, it follows that only TROB₁ is nonzero. The addition of the spin-orbit coupling introduces interband triplet

pairing, and the second term in Eq. (35) for TROB₂ is therefore nonzero.

V. CONCLUSIONS AND OUTLOOK

Motivated by the observation of the polar Kerr effect in chiral-superconductor candidate materials, in this paper we have considered the origin of the anomalous Hall conductivity in a general model of a two-band superconductor. Our analysis reveals a key role for two distinct gauge-invariant time-reversal-odd bilinear functions (TROBs) of the pairing potential: if at least one of these TROBs is present, we may generically expect that the anomalous Hall conductivity is nonzero. Although our result is rigorously valid in the high-frequency, small-gap limit, we argued that it applies more generally. The TROBs strongly constrain the form of the pairing potential that generates an anomalous Hall conductivity. Explicitly calculating the TROBs in a pseudospin-band basis, we found that interband pairing generically gives rise to an anomalous Hall conductivity, but also demonstrated that purely intraband nonunitary triplet pairing can make a contribution. Our general conclusions are illustrated with three specific examples involving chiral p -wave and d -wave superconductors.

For the purposes of analytical clarity, our study has been restricted to a model with a twofold orbital degree of freedom. It nevertheless appears straightforward to generalize our analysis to systems with more orbital degrees of freedom. For example, more realistic models of the low-energy electronic structure of Sr_2RuO_4 typically involve at least three bands [21,22,24,28,46]. We speculate that in a system with n orbital degrees of freedom there will be n distinct TROBs; this follows from the observation that the normal state Hamiltonian $H_0(\mathbf{k})$ of such a system obeys the characteristic polynomial

$$\prod_{j=1}^n [H_0(\mathbf{k}) - E_{k,j}] = 0, \quad (51)$$

where $E_{k,j}$ are the n distinct doubly degenerate eigenvalues of the normal state. This implies that we can define n independent TROBs

$$\text{TROB}_j = \tilde{\Delta} \tilde{H}_0^{j-1} \tilde{\Delta}^\dagger - \tilde{\Delta}^\dagger \tilde{H}_0^{j-1} \tilde{\Delta}, \quad (52)$$

where \tilde{H}_0 is the traceless part of H_0 . Due to the characteristic polynomial Eq. (51), TROBs defined in terms of powers of H_0 higher than $n - 1$ can be expressed in terms of $\text{TROB}_{j=1,\dots,n}$. We leave a detailed analysis of this situation to future work.

Further generalization of our results should consider going beyond the small-gap limit, to explore the relevance of TROBs at all energy scales. Another direction for future work is to extend our argument to noncentrosymmetric systems, which could be relevant to time-reversal symmetry-breaking candidate superconductors LaNiC_2 [47] and twisted bilayer graphene [6].

ACKNOWLEDGMENT

This work was supported by the Marsden Fund Council from Government funding, managed by Royal Society Te Apārangi.

- [1] C. Kallin and J. Berlinsky, Chiral superconductors, *Rep. Prog. Phys.* **79**, 054502 (2016).
- [2] A. P. Mackenzie and Y. Maeno, The superconductivity of Sr_2RuO_4 and the physics of spin-triplet pairing, *Rev. Mod. Phys.* **75**, 657 (2003).
- [3] M. Norman, What is the superconducting order parameter for UPt_3 ?, *Physica C: Superconduct.* **194**, 203 (1992).
- [4] R. Joynt and L. Taillefer, The superconducting phases of UPt_3 , *Rev. Mod. Phys.* **74**, 235 (2002).
- [5] Y. Kasahara, T. Iwasawa, H. Shishido, T. Shibauchi, K. Behnia, Y. Haga, T. D. Matsuda, Y. Onuki, M. Sigrist, and Y. Matsuda, Exotic Superconducting Properties in the Electron-Hole-Compensated Heavy-Fermion “Semimetal” URu_2Si_2 , *Phys. Rev. Lett.* **99**, 116402 (2007).
- [6] Y. Cao, V. Fatemi, S. Fang, K. Watanabe, T. Taniguchi, E. Kaxiras, and P. Jarillo-Herrero, Unconventional superconductivity in magic-angle graphene superlattices, *Nature (London)* **556**, 43 (2018).
- [7] P. N. Argyres, Theory of the Faraday and Kerr Effects in Ferromagnetics, *Phys. Rev.* **97**, 334 (1955).
- [8] A. Kapitulnik, J. Xia, E. Schemm, and A. Palevski, Polar Kerr effect as probe for time-reversal symmetry breaking in unconventional superconductors, *New J. Phys.* **11**, 055060 (2009).
- [9] J. Xia, Y. Maeno, P. T. Beyersdorf, M. M. Fejer, and A. Kapitulnik, High Resolution Polar Kerr Effect Measurements of Sr_2RuO_4 : Evidence for Broken Time-Reversal Symmetry in the Superconducting State, *Phys. Rev. Lett.* **97**, 167002 (2006).
- [10] E. R. Schemm, W. J. Gannon, C. M. Wishne, W. P. Halperin, and A. Kapitulnik, Observation of broken time-reversal symmetry in the heavy-fermion superconductor UPt_3 , *Science* **345**, 190 (2014).
- [11] E. R. Schemm, R. E. Baumbach, P. H. Tobash, F. Ronning, E. D. Bauer, and A. Kapitulnik, Evidence for broken time-reversal symmetry in the superconducting phase of URu_2Si_2 , *Phys. Rev. B* **91**, 140506(R) (2015).
- [12] X. Gong, M. Kargarian, A. Stern, D. Yue, H. Zhou, X. Jin, V. M. Galitski, V. M. Yakovenko, and J. Xia, Time-reversal symmetry-breaking superconductivity in epitaxial bismuth/nickel bilayers, *Sci. Adv.* **3**, 1602579 (2017).
- [13] E. M. Levenson-Falk, E. R. Schemm, Y. Aoki, M. B. Maple, and A. Kapitulnik, Polar Kerr Effect from Time-Reversal Symmetry Breaking in the Heavy-Fermion Superconductor $\text{PrOs}_4\text{Sb}_{12}$, *Phys. Rev. Lett.* **120**, 187004 (2018).
- [14] I. M. Hayes, D. S. Wei, T. Metz, J. Zhang, Y. S. Eo, S. Ran, S. R. Saha, J. Collini, N. P. Butch, D. F. Agterberg, A. Kapitulnik, and J. Paglione, Weyl superconductivity in UTe_2 , *arXiv:2002.02539*.
- [15] E. Taylor and C. Kallin, Intrinsic Hall Effect in a Multiband Chiral Superconductor in the Absence of an External Magnetic Field, *Phys. Rev. Lett.* **108**, 157001 (2012).
- [16] E. J. König and A. Levchenko, Kerr Effect from Diffractive Skew Scattering in Chiral $p_x \pm ip_y$ Superconductors, *Phys. Rev. Lett.* **118**, 027001 (2017).
- [17] J. Goryo, Impurity-induced polar Kerr effect in a chiral p -wave superconductor, *Phys. Rev. B* **78**, 060501(R) (2008).
- [18] R. M. Lutchyn, P. Nagornykh, and V. M. Yakovenko, Frequency and temperature dependence of the anomalous ac Hall conductivity in a chiral $p_x + ip_y$ superconductor with impurities, *Phys. Rev. B* **80**, 104508 (2009).
- [19] S. Li, A. V. Andreev, and B. Z. Spivak, Anomalous transport phenomena in $p_x + ip_y$ superconductors, *Phys. Rev. B* **92**, 100506(R) (2015).
- [20] Y. Li, Z. Wang, and W. Huang, Anomalous Hall effect in chiral superconductors from impurity superlattices, *Phys. Rev. Res.* **2**, 042027(R) (2020).
- [21] K. I. Wysokiński, J. F. Annett, and B. L. Györfly, Intrinsic Optical Dichroism in the Chiral Superconducting State of Sr_2RuO_4 , *Phys. Rev. Lett.* **108**, 077004 (2012).
- [22] M. Gradhand, K. I. Wysokiński, J. F. Annett, and B. L. Györfly, Kerr rotation in the unconventional superconductor Sr_2RuO_4 , *Phys. Rev. B* **88**, 094504 (2013).
- [23] Z. Wang, J. Berlinsky, G. Zwicknagl, and C. Kallin, Intrinsic ac anomalous Hall effect of nonsymmorphic chiral superconductors with an application to UPt_3 , *Phys. Rev. B* **96**, 174511 (2017).
- [24] J. Robbins, J. F. Annett, and M. Gradhand, Effect of spin-orbit coupling on the polar Kerr effect in Sr_2RuO_4 , *Phys. Rev. B* **96**, 144503 (2017).
- [25] J. Robert and W. Wen-Chin, Superconductivity in empty bands and multiple order parameter chirality, *Sci. Rep.* **7**, 12968 (2017).
- [26] C. Triola and A. M. Black-Schaffer, Odd-frequency pairing and Kerr effect in the heavy-fermion superconductor UPt_3 , *Phys. Rev. B* **97**, 064505 (2018).
- [27] P. M. R. Brydon, D. S. L. Abergel, D. F. Agterberg, and V. M. Yakovenko, Loop Currents and Anomalous Hall Effect from Time-Reversal Symmetry-Breaking Superconductivity on the Honeycomb Lattice, *Phys. Rev. X* **9**, 031025 (2019).
- [28] J.-L. Zhang, Y. Li, W. Huang, and F.-C. Zhang, Hidden anomalous Hall effect in Sr_2RuO_4 with chiral superconductivity dominated by the Rud_{xy} orbital, *Phys. Rev. B* **102**, 180509(R) (2020).
- [29] S. Yip, Pseudospin bases for a model of $\text{Cu} : \text{Bi}_2\text{Se}_3$, *arXiv:1609.04152*.
- [30] J. W. F. Venderbos, V. Kozii, and L. Fu, Odd-parity superconductors with two-component order parameters: Nematic and chiral, full gap, and Majorana node, *Phys. Rev. B* **94**, 180504(R) (2016).
- [31] G. D. Mahan, *Many-Particle Physics*, 3rd ed. (Springer, Berlin, 1980).
- [32] A. Ramires, D. F. Agterberg, and M. Sigrist, Tailoring T_c by symmetry principles: The concept of superconducting fitness, *Phys. Rev. B* **98**, 024501 (2018).
- [33] P. M. R. Brydon, D. F. Agterberg, H. Menke, and C. Timm, Bogoliubov fermi surfaces: General theory, magnetic order, and topology, *Phys. Rev. B* **98**, 224509 (2018).
- [34] G. M. Luke, Y. Fudamoto, K. M. Kojima, M. I. Larkin, J. Merrin, B. Nachumi, Y. J. Uemura, Y. Maeno, Z. Q. Mao, Y. Mori, H. Nakamura, and M. Sigrist, Time-reversal symmetry-breaking superconductivity in Sr_2RuO_4 , *Nature (London)* **394**, 558 (1998).
- [35] K. Ishida, H. Mukuda, Y. Kitaoka, K. Asayama, Z. Q. Mao, Y. Mori, and Y. Maeno, Spin-triplet superconductivity in Sr_2RuO_4 identified by ^{17}O knight shift, *Nature (London)* **396**, 658 (1998).
- [36] J. A. Duffy, S. M. Hayden, Y. Maeno, Z. Q. Mao, J. Kulda, and G. J. McIntyre, Polarized-Neutron Scattering Study of the Cooper-Pair Moment in Sr_2RuO_4 , *Phys. Rev. Lett.* **85**, 5412 (2000).

- [37] K. Ishida, H. Mukuda, Y. Kitaoka, Z. Q. Mao, H. Fukazawa, and Y. Maeno, Ru NMR probe of spin susceptibility in the superconducting state of Sr_2RuO_4 , *Phys. Rev. B* **63**, 060507(R) (2001).
- [38] A. Pustogow, Y. Luo, A. Chronister, Y.-S. Su, D. A. Sokolov, F. Jerzembeck, A. P. Mackenzie, C. W. Hicks, N. Kikugawa, S. Raghu, E. D. Bauer, and S. E. Brown, Constraints on the superconducting order parameter in Sr_2RuO_4 from oxygen-17 nuclear magnetic resonance, *Nature (London)* **574**, 72 (2019).
- [39] K. Ishida, M. Manago, K. Kinjo, and Y. Maeno, Reduction of the ^{17}O Knight shift in the superconducting state and the heat-up effect by NMR pulses on Sr_2RuO_4 , *J. Phys. Soc. Jpn.* **89**, 034712 (2020).
- [40] A. Tamai, M. Zingl, E. Rozbicki, E. Cappelli, S. Riccò, A. de la Torre, S. McKeown Walker, F. Y. Bruno, P. D. C. King, W. Meevasana, M. Shi, M. Radović, N. C. Plumb, A. S. Gibbs, A. P. Mackenzie, C. Berthod, H. U. R. Strand, M. Kim, A. Georges, and F. Baumberger, High-Resolution Photoemission on Sr_2RuO_4 Reveals Correlation-Enhanced Effective Spin-Orbit Coupling and Dominantly Local Self-Energies, *Phys. Rev. X* **9**, 021048 (2019).
- [41] E. J. Rozbicki, J. F. Annett, J.-R. Souquet, and A. P. Mackenzie, Spin-orbit coupling and k -dependent Zeeman splitting in strontium ruthenate, *J. Phys.: Condens. Matter* **23**, 094201 (2011).
- [42] M. W. Haverkort, I. S. Elfimov, L. H. Tjeng, G. A. Sawatzky, and A. Damascelli, Strong Spin-Orbit Coupling Effects on the Fermi Surface of Sr_2RuO_4 and Sr_2RhO_4 , *Phys. Rev. Lett.* **101**, 026406 (2008).
- [43] A. M. Black-Schaffer and S. Doniach, Resonating valence bonds and mean-field d -wave superconductivity in graphite, *Phys. Rev. B* **75**, 134512 (2007).
- [44] W. Wu, M. M. Scherer, C. Honerkamp, and K. Le Hur, Correlated Dirac particles and superconductivity on the honeycomb lattice, *Phys. Rev. B* **87**, 094521 (2013).
- [45] C. L. Kane and E. J. Mele, Quantum Spin Hall Effect in Graphene, *Phys. Rev. Lett.* **95**, 226801 (2005).
- [46] H. G. Suh, H. Menke, P. M. R. Brydon, C. Timm, A. Ramires, and D. F. Agterberg, Stabilizing even-parity chiral superconductivity in Sr_2RuO_4 , *Phys. Rev. Res.* **2**, 032023(R) (2020).
- [47] A. D. Hillier, J. Quintanilla, and R. Cywinski, Evidence for Time-Reversal Symmetry Breaking in the Noncentrosymmetric Superconductor LaNiC_2 , *Phys. Rev. Lett.* **102**, 117007 (2009).